9

Research Article

Walid Ali Rahoma*, Akram Masoud, Fawzy Ahmed Abd El-Salam, and Elamira Hend Khattab

Perturbed locations and linear stability of collinear Lagrangian points in the elliptic restricted three body problem with triaxial primaries

https://doi.org/10.1515/astro-2019-0013 Received Oct 21, 2017; accepted Aug 20, 2018

Abstract: This paper aims to study the effect of the triaxiality and the oblateness as a special case of primaries on the locations and stability of the collinear equilibrium points of the elliptic restricted three body problem (in brief ERTBP). The locations of the perturbed collinear equilibrium points are first determined in terms of mass ratio of the problem (the smallest mass divided by the total mass of the system) and different concerned perturbing factors. The difference between the locations of collinear points in the classical case of circular restricted three body problem and those in the perturbed case is represented versus mass ratio over its range. The linear stability of the collinear points is discussed. It is observed that the stability regions for our model depend mainly on the eccentricity of the orbits in addition to the considered perturbations.

Keywords: ERTBP, Collinear pionts, Oblateness, Triaxiality, Stability

1 Introduction

The general three-body problem is described as a third body of infinitesimal mass m_3 that is attracted by two finite masses called primaries but not influencing their motion, moves in the plane defined by the two revolving primaries. The primaries are of arbitrary masses m_1 and m_2 and revolve around their center of mass in circular orbits (this system denoted briefly, CRTBP), see for instance, the fundamental celestial mechanics books, *e.g.* Szebehely (1976) and Murray and Drmott (1999). For more generalization, it is supposed that the primaries revolve around common center of mass in elliptical orbits (this system denoted briefly, ERTBP). ERTBP appears a more difficulty involved in handling it. Even if the CRTBP is not integrable, a number of special solutions can be found. The points where the third body has zero velocity and zero acceleration in the rotating

frame are special solutions. Such points are called equilibrium points. The position of the infinitesimal body is displaced a little from the equilibrium point due to the some perturbations. If the resultant motion of the infinitesimal mass is a rapid departure from the vicinity of the point, we can call such a position of equilibrium point an "unstable one", if however the body merely oscillates about the equilibrium point, it is said to be a "stable position" (in the sense of Lyapunov), Abd El-Salam (2015). In general case, the dynamics of circular and/or elliptical three-body problem has a wide applications in astrophysics for example but not all stellar/solar system dynamics and Earth-Moon system. So this problem received more attention from the astronomers and dynamical system scientists and can't be enumerated. in spite of it, the solutions of this problem has been developed over the past centuries.

The scientific history of the restricted three-body problem is very wealth to be mentioned but here is the most related and recent studies dealt with CRTBP as well as ERTBP with and without considering different perturbations Sharma (1987), Tsirogiannis *et al.* (2006); Kushvah and Ishwar (2006); Vishnu Namboori *et al.* (2008); Mital *et al.* (2009); Singh and Ishwar (1999); Kumar and Ishwar (2009); Rahoma and Abd El-Salam (2014); Rahoma (2016) and references therein.

Corresponding Author: W. A. Rahoma: Department of Astronomy, Faculty of Science, Cairo University, Cairo,12613, Egypt; Email: rahoma@sci.cu.edu.eg

Akram Masoud, E. H. Khattab: Department of Astronomy, Faculty of Science, Cairo University, Cairo,12613, Egypt

F. A. Abd El-Salam: Department of Astronomy, Faculty of Science, Cairo University, Cairo,12613, Egypt; Department of Mathematics, Faculty of Science, Taibah University, Madina, KSA

∂ Open Access. © 2019 W. A. Rahoma *et al. et al.*, published by De Gruyter. Attribution 4.0 License



It seems good to present some of the important related works focused on the ERTBP, Sharma et al. (2001) analyzed the equilibrium points stability retrieved that the triangular quilibrium points are stable conditionally but collinear points are always unstable. Ammar (2008) analyzed solar radiation pressure effect on the positions and stability of the libration points in ERTBP. Singh (2011) formulated the triangular libration points nonlinear stability under the effect Coriolis and centrifugal forces as small perturbations in addition to the effect of primaries oblateness and radiation pressures. Singh and Umar (2012) investigated the stability of triangular equilibrium points in the ERTBP, considering both primaries are oblate and emit light energy simultaneously. Singh and Umar (2013) investigated the luminous and oblate spheroids of primaries effect on the locations and stability of the collinear libration points. In another work, Singh and Umar (2014) studied the effect of the big primary's triaxial and a spherical shape of the companion on the locations and stability of the collinear libration points. They found that the position of collinear libration points and their stability are affected with their considered perturbations in addition to the eccentricity and the semi-major axis of the primaries orbit as well.

Katour *et al.* (2014); Singh and Bello (2014a,b, 2015a,b); Abd El-Salam and Abd El-Bar (2015); Abd El-Bar *et al.* (2015) and Bello and Singh (2016) concerned with the relativistic R3BP in addition to some different perturbations; the primaries oblateness, radiation from one of the primaries, upon the equilibrium points locations and stability. They noticed that the stability regions of the their concerned equilibrium points are varied (expanding or shrinking) related to the critical mass value and depending upon the value of their considered perturbations.

In recent works, the calculations of the effect of different perturbations like oblateness, ellipsoidal primaries and photogravitational relativistic on the equilibrium points locations and its stability in the restricted three-body problem are investigated, Wang *et al.* (2018); Wu *et al.* (2018); Abd El-Salam and Abd El-Bar (2018) and Xin and Hou (2017). They concluded that the collinear points stability is highly affected at a whole range of mass, contrary to the stability regions of the triangular points which are affected differently depend on the perturbations kind.

The aim of this study is the determination of the locations of the collinear equilibrium points and investigating their linear stability in the ERTBP taking into consideration both primaries triaxial. The oblateness is discussed as a special case of triaxiality. This aim comes as a continuation study for a previously started work by Abd El-Salam (2015). The equations of ERTBP is not adequate easy to dealing with because the Hamiltonian of the problem be-

comes time-dependent. Utilizing from the pulsating and non-uniformly rotating coordinate reference frame, the system can be brought to a form where the primaries positions become at fixed and the infinitesimal body motion can be analyzed relative to their locations.

This paper will be organized after this introduction section as follows: the equation of motion in ERTBP with oblate and triaxial primaries will be formulated in section 2, the computations related to the location of equilibrium points in ERTBP with the considered perturbations will be introduced in section 3. Sec. 4 highlighted the small displacement effect of a test particle located in collinear points. In sec. 5 all the computations related to the stability of collinear points are introduced. Finally a numerical simulations are presented in sec. 6 with discussion and a work conclusion is shown in sec. 7.

2 Equations of motion

The motion of an infinitesimal particle in the ERTBP with oblate and triaxial primaries in a dimensionless, barycentric and pulsating rotating coordinate system (ξ , η) is described by Abd El-Salam (2015)

$$\frac{d^2\xi}{df^2} - 2\frac{d\eta}{df} = (1 + e\cos f)^{-1}\frac{\partial U}{\partial \xi}$$
 (1)

$$\frac{d^2\eta}{df^2} + 2\frac{d\xi}{df} = (1 + e\cos f)^{-1}\frac{\partial U}{\partial n}$$
 (2)

With the potential-like function U given by

$$U = \frac{1}{2} \left[(1 - \mu) r_1^2 + \mu r_2^2 \right] + \frac{1}{n^2} \left(\frac{1 - \mu}{r_1} + \frac{\mu}{r_2} \right)$$
(3)

$$+ \frac{1}{2n^2} \left(A_\sigma \frac{1 - \mu}{r_1^3} + A_y \frac{\mu}{r_2^3} \right)$$

where f is the true anomaly of the more massive primary, m_1 , e is the eccentricity of any primary's orbit, μ is the ratio of the mass of smaller primary to the total mass of the primaries and it satisfies $0 < \mu \le 1/2$, n is the mean motion, $A_{\sigma} = A_1 + (2\sigma_1 - \sigma_2)$ and $A_y = A_2 + (2y_1 - y_2)$ are the total averaged oblateness and triaxiality coefficients for larger and smaller primaries respectively. $A_1, A_2, (2\sigma_1 - \sigma_2)$ and $(2y_1 - y_2)$ are the oblateness and triaxiality factors for larger and smaller primaries respectively. r_1 and r_2 , the distances of the infinitesimal mass from larger and smaller primaries respectively are given by.

$$r_1 = \sqrt{(\xi + \mu)^2 + \eta^2}$$

$$r_2 = \sqrt{(\xi + \mu - 1)^2 + \eta^2}$$

Finally the mean motion of the system is given by

$$n^2 = \frac{1}{a\left(1-e^2\right)}\left(1+\frac{3}{2}A_\sigma + \frac{3}{2}A_y\right)$$

3 Existence of the collinear equilibrium points

Since the equilibrium points have zero relative velocities and zero relative accelerations, then the locations of them is determined by equating the partial derivatives of the potential-like function to zero,

$$\frac{\partial U}{\partial \xi} = \frac{\partial U}{\partial \eta} = 0 \tag{4}$$

where

DE GRUYTER

$$n^{2}\xi - \frac{(1-\mu)(\xi+\mu)}{r_{1}^{3}} - \frac{3}{2}A_{\sigma}\frac{(1-\mu)(\xi+\mu)}{r_{1}^{5}}$$

$$-\frac{\mu(\xi+\mu-1)}{r_{2}^{3}} - \frac{3}{2}A_{y}\frac{\mu(\xi+\mu-1)}{r_{2}^{5}} = 0$$
(5)

and

$$n^2 \eta - \left(\frac{1-\mu}{r_1^3} + \frac{3}{2} A_\sigma \frac{(1-\mu)}{r_1^5} + \frac{\mu}{r_2^3} + \frac{3}{2} A_y \frac{\mu}{r_2^5}\right) \eta = 0 \quad (6)$$

The solutions of the Eqs. (5-6) with $\eta = 0$ give the location of the triangular equilibrium points L_4 and L_5 whereas the trivial solution $\eta = 0$ gives the location of the collinear equilibrium points L_1 , L_2 and L_3 which are the cases of our study. Ignoring the perturbing coefficients in Eqs. (5-6), oblateness, triaxiality and ellipticity, The system will be retrieved to CRTBP system.

4 Linear stability analysis

To study the stability of the equilibrium points, a small displacement is occurred to a test particle located in those points due to the included perturbations. We will call the point a "stable position" if the body simply oscillates around the equilibrium point, also the point can be called as an "unstable one" if the body leavs rapidly from the point neighborhood; in the Lyapunov sense. In order to study the effect of a small displacement on a test particle subjected on the equilibrium collinear points, the equations of motion must be linearized around these points. Similarity transformation technique is used in order to solve the system of linear differential equation resulted from the linearization process. Consider a small displacement $(\mathfrak{X}, \mathfrak{Y})$ from the

collinear equilibrium points (ξ_i, η_i) , i = 1, 2, 3 such that $\xi = \xi_i + \mathcal{X}$ and $\eta = \eta_i + \mathcal{Y}$, the linearized equation can be expressed as

$$\mathcal{X}_{ff} - 2\mathcal{Y}_f = \mathcal{F}\left\{\mathcal{X}\ U_{\xi\xi}^{(L_i)} + \mathcal{Y}\ U_{\xi\eta}^{(L_i)}\right\},\tag{7}$$

$$\mathcal{Y}_{ff} + 2\mathcal{X}_{f} = \mathcal{F}\left\{\mathcal{X} U_{\xi\eta}^{L_{i}} + \mathcal{Y} U_{\eta\eta}^{L_{i}}\right\}, \tag{8}$$

$$U_{\xi\xi}^{(L_{i})} = 1 + \frac{2}{n^{2}} \left(\frac{1 - \mu}{|\xi_{i} + \mu|^{3}} + \frac{\mu}{|\xi_{i} + \mu - 1|^{3}} \right) + \frac{6}{n^{2}} \left(A_{\sigma} \frac{1 - \mu}{|\xi_{i} + \mu|^{5}} + A_{y} \frac{\mu}{|\xi_{i} + \mu - 1|^{5}} \right),$$
(9)

$$U_{\eta\eta}^{(L_{i})} = 1 - \frac{1}{n^{2}} \left(\frac{1 - \mu}{|\xi_{i} + \mu|^{3}} + \frac{\mu}{|\xi_{i} + \mu - 1|^{3}} \right)$$

$$- \frac{3}{2n^{2}} \left(A_{\sigma} \frac{1 - \mu}{|\xi_{i} + \mu|^{5}} + A_{y} \frac{\mu}{|\xi_{i} + \mu - 1|^{5}} \right),$$
(10)

$$U_{\xi n}^{(L_i)} = 0 \tag{11}$$

Where $\mathcal{F} = (1 + e \cos f)^{-1}$, \mathcal{X}_f , \mathcal{X}_{ff} , \mathcal{Y}_f and \mathcal{Y}_{ff} are the partial derivatives of the small displacement with respect to true anomaly f and $U_{\xi}^{(L_i)}$, $U_{\xi\xi}^{(L_i)}$, $U_{\eta}^{(L_i)}$, $U_{\eta\eta}^{(L_i)}$ and $U_{\xi\eta}^{(L_i)}$ are the partial derivatives of the potential-like function at the equilibrium point L_i , i = 1, 2, 3. The general solution of the linearized equation is

$$\mathcal{X} = \sum_{j=1}^{4} \alpha_j e^{\lambda_j f}, \quad \mathcal{Y} = \sum_{j=1}^{4} \beta_j e^{\lambda_j f}$$
 (12)

where λ_i are the characteristic roots, which can be evaluated from the corresponding characteristic equation

$$\lambda^4 + \mathcal{U}_{I,i}\lambda^2 + \mathcal{V}_{I,i} = 0 \tag{13}$$

where

$$\mathcal{U}_{L_i} = 4 - \mathcal{F}\left(U_{\xi\xi}^{(L_i)} + U_{\eta\eta}^{(L_i)}\right) \tag{14}$$

$$V_{L_i} = \mathcal{F}^2 U_{\xi\xi}^{(L_i)} U_{\eta\eta}^{(L_i)}$$
 (15)

Also α_i and β_i are dependent constants and they are defined as

$$\beta_j = \frac{\lambda_j^2 - \mathcal{F}U_{\xi\xi}^{(L_i)}}{2\lambda_i} \alpha_j \tag{16}$$

By meditation at Eq. (12), the positive eigenvalue gives rise to exponential growth that lead to instability case whereas

the imaginary eigenvalue gives rise to oscillation terms that lead to stability case. The exponential decay is resulted from negative eigenvalue. However, from Eq. (13) the negative eigenvalue is resulted together with positive one from the equation.

$$\lambda_{1,2} = \pm \frac{1}{\sqrt{2}} \sqrt{-\mathcal{U}_{L_i} - \sqrt{(\mathcal{U}_{L_i})^2 - 4\mathcal{V}_{L_i}}},$$

$$\lambda_{3,4} = \pm \frac{1}{\sqrt{2}} \sqrt{-\mathcal{U}_{L_i} + \sqrt{(\mathcal{U}_{L_i})^2 - 4\mathcal{V}_{L_i}}}$$
(17)

It is clear that $\lambda_1 = -\lambda_2$ and $\lambda_3 = -\lambda_4$, then at the stable points, the roots of the characteristic equation must satisfy $\lambda_1^2 = \lambda_2^2 < 0$ and $\lambda_3^2 = \lambda_4^2 < 0$. This implies that for stability case the following sufficient and necessary conditions should be satisfied simultaneously

$$U_{\xi\xi}^{(L_i)}U_{\eta\eta}^{(L_i)} > 0, \quad U_{\xi\xi}^{(L_i)} + U_{\eta\eta}^{(L_i)} < \frac{4}{\mathcal{F}}$$
 (18)

5 Perturbed locations of Lagrangian points

The location of collinear Lagrangian points in the case of CRTBP is determined in many textbooks of celestial mechanics, *e.g.* ?. In this section, the required computation is to determine the locations of these collinear libration points in ERTBP with oblate and triaxial primaries. These new locations will be obtained as a perturbation of CRTBP Lagrangian points' locations as follows.

5.1 Location of L_1

The location of L_1 in the case of CRTBP is determined by the following power series,

$$R_1 = 1 - \alpha + \frac{1}{3}\alpha^2 + \frac{1}{9}\alpha^3 + \frac{23}{81}\alpha^4 + \mathcal{O}\left[\alpha^5\right]$$
 (19)

with $R_1+R_2=1$, $\alpha=\left[\frac{\mu}{3(1-\mu)}\right]^{1/3}$ where R_1 and R_2 are the positions of L_1 with respect to m_1 and m_2 , respectively. In the case of ERTBP with oblatness and triaxiality case, R_1 and R_2 will be slightly changed due to the perturbations in addition to ellipticity of the primaries orbit,

$$r_1 = R_1 + \varepsilon_1, \quad r_2 = R_2 + \varepsilon_2 \tag{20}$$

where ε_1 and ε_2 are small perturbations factors. For the case of perturbed first Lagrangian point $L_1(\xi_1, 0)$ we have

$$r_1 = \xi_1 + \mu, \quad r_2 = 1 - \xi_1 - \mu$$
 (21)

Denote $\varepsilon_1 = \varepsilon$ and $R_1 = R$ then using Eq. (20) and Eq. (21) yields

$$\begin{cases}
\xi_1 = R - \mu + \varepsilon \\
r_1 = R + \varepsilon \\
r_2 = [1 - R] - \varepsilon
\end{cases}$$
(22)

Substitute Eq. (22) into Eq. (5) yields

$$n^{2} [R - \mu + \varepsilon] - (1 - \mu) [R + \varepsilon]^{-2} - \frac{3}{2} A_{\sigma} (1 - \mu) [R + \varepsilon]^{-4}$$
$$+ \mu [[1 - R] - \varepsilon]^{-2} + \frac{3}{2} A_{y} \mu [[1 - R] - \varepsilon]^{-4} = 0$$

This equation can be written as

$$n^{2} [R - \mu + \varepsilon] - (1 - \mu) \left\{ R \left[1 + \frac{\varepsilon}{R} \right] \right\}^{-2}$$

$$(18) \quad -\frac{3}{2} A_{\sigma} (1 - \mu) \left\{ R \left[1 + \frac{\varepsilon}{R} \right] \right\}^{-4} + \mu \left\{ [1 - R] \left[1 - \frac{\varepsilon}{1 - R} \right] \right\}^{-2}$$

$$+ \frac{3}{2} A_{y} \mu \left\{ [1 - R] \left[1 - \frac{\varepsilon}{1 - R} \right] \right\}^{-4} = 0$$

Since $\frac{\varepsilon}{R} << 1$, $\frac{\varepsilon}{1-R} << 1$ then we can use the Maclaurin formula $(1 \pm M)^m \ 1 \pm mM$

$$n^{2} [R - \mu + \varepsilon] - (1 - \mu) R^{-2} \left[1 - 2 \frac{\varepsilon}{R} \right]$$

$$- \frac{3}{2} A_{\sigma} (1 - \mu) R^{-4} \left[1 - 4 \frac{\varepsilon}{R} \right] + \mu [1 - R]^{-2} \left[1 + 2 \frac{\varepsilon}{1 - R} \right]$$

$$+ \frac{3}{2} A_{y} \mu [1 - R]^{-4} \left[1 + 4 \frac{\varepsilon}{1 - R} \right] = 0$$

The solution will be

$$\varepsilon = \frac{n^{2} \left[\mu - R\right] + \left\{\frac{1-\mu}{R^{2}} - \frac{\mu}{\left[1-R\right]^{2}}\right\} + \frac{3}{2} \left\{A_{\sigma} \frac{1-\mu}{R^{4}} - A_{\gamma} \frac{\mu}{\left[1-R\right]^{4}}\right\}}{n^{2} + 2\left\{\frac{1-\mu}{R^{3}} + \frac{\mu}{\left[1-R\right]^{3}}\right\} + 6\left\{A_{\sigma} \frac{1-\mu}{R^{5}} + A_{\gamma} \frac{\mu}{\left[1-R\right]^{5}}\right\}}$$

Provided

$$n^{2} + 2\left\{\frac{1-\mu}{R^{3}} + \frac{\mu}{[1-R]^{3}}\right\} + 6\left\{A_{\sigma}\frac{1-\mu}{R^{5}} + A_{y}\frac{\mu}{[1-R]^{5}}\right\} \neq 0$$
(24)

By looking at Eq. (23), we find that ε equals to the negative ratio of the first partial derivative of the potential-like function with respect to ξ at $r_1 = R_1 = R$ of non perturbed location of L_1 to that the second partial derivative of the potential-like function with respect to the same variable at $r_1 = R_1 = R$, *i.e.*

$$\varepsilon = -\frac{U_{\xi}^{[R]}}{U_{\xi\xi}^{[R]}}, \qquad \qquad U_{\xi\xi}^{[R]} \neq 0$$
 (25)

Then the perturbed location of L_1 can be expressed as,

$$\begin{pmatrix}
R - \mu - \frac{U_{\xi}^{[R]}}{U_{\xi\xi}^{[R]}}, 0 \\
U_{\xi\xi}^{[R]} \neq 0
\end{pmatrix},$$

$$R = 1 - \alpha + \frac{1}{3}\alpha^{2} + \frac{1}{9}\alpha^{3} + \frac{23}{81}\alpha^{4} + \mathcal{O}\left[\alpha^{5}\right],$$

$$\alpha = \left[\frac{\mu}{3(1-\mu)}\right]^{1/3}$$
(26)

Removing all oblatness and triaxility factors for both Larger and smaller primaries (A_{σ} , $A_{y} \rightarrow 0$) also remove the ellipticity factor ($n \rightarrow 1$), the perturbation factor will approach to zero, i.e.,

$$\lim_{(n,A_{\sigma},A_{\nu})\to(1,0,0)} \varepsilon = 0$$
 (27)

Which confirms the unperturbed location obtained, see Eq. (19).

5.2 Location of L_2

DE GRUYTER

The location of L_2 in the case of CRTBP can be determined as

$$R_1 = 1 + \alpha + \frac{1}{3}\alpha^2 - \frac{1}{9}\alpha^3 - \frac{31}{81}\alpha^4 + \mathcal{O}\left[\alpha^5\right]$$
 (28)

with $R_1 - R_2 = 1$, $\alpha = (\frac{\mu}{3(1-\nu)})^{1/3}$, where R_1 and R_2 are the positions of L_2 with respect to m_1 and m_2 . Similar to L_1 , the perturbation factor can be expressed as

$$\varepsilon = -\frac{U_{\xi}^{[R]}}{U_{\xi\xi}^{[R]}}, \quad U_{\xi\xi}^{[R]} \neq 0$$
 (29)

The formal coordinate of L_2 will be formulated as:

$$\begin{pmatrix}
R - \mu - \frac{U_{\xi}^{[R]}}{U_{\xi\xi}^{[R]}} \varepsilon, 0 \\
U_{\xi\xi}^{[R]} \neq 0
\end{pmatrix},$$

$$R = 1 + \alpha + \frac{1}{3}\alpha^2 - \frac{1}{9}\alpha^3 - \frac{31}{81}\alpha^4 + \mathcal{O}\left[\alpha^5\right],$$

$$\alpha = \left[\frac{\mu}{3(1-\mu)}\right]^{1/3}$$
(30)

Removing all perturbations, the location of L_2 will be retrieved to its position in CRTBP

$$\lim_{(n,A_{\sigma},A_{\gamma})\to(1,0,0)} \varepsilon = 0 \tag{31}$$

Which confirms again the unperturbed location obtained, see Eq. (28).

5.3 Location of L_3

The location of L_3 in the case of CRTBP can be determined

$$R_1 = R_1 = 1 - \frac{7}{12}\alpha + \frac{7}{12}\alpha^2 - \frac{13223}{20736}\alpha^3 + \mathcal{O}\left[\alpha^4\right]$$
 (32)

with $R_2 - R_1 = 1$, $\alpha = \frac{\mu}{(1-\mu)}$ where R_1 and R_2 are the positions of L_3 with respect to m_1 and m_2 . Similar to the previous cases,

$$\varepsilon = \frac{U_{\xi}^{[R]}}{U_{\xi\xi}^{[R]}}, \quad U_{\xi\xi}^{[R]} \neq 0$$
(33)

The coordinates of L_3 will be

$$\begin{pmatrix}
-R - \mu - \frac{U_{\xi}^{[R]}}{U_{\xi\xi}^{[R]}}, 0 \\
0 \\
U_{\xi\xi}^{[R]} \neq 0 \\
R = 1 - \frac{7}{12}\alpha + \frac{7}{12}\alpha^2 - \frac{13223}{20736}\alpha^3 + \mathcal{O}\left[\alpha^4\right], \\
\alpha = \frac{\mu}{(1 - \mu)}
\end{pmatrix} (34)$$

$$\lim_{(n,A_{\sigma},A_{\gamma})\to(1,0,0)} \varepsilon = 0 \tag{35}$$

Which confirms again the unperturbed location obtained, see Eq. (32).

Graphical representation and analysis

In this section we will use the numerical values of the included parameters listed in Table 1 to introduce some graphical representations illustrating the effect of the considered perturbation on:

- 1. The locations of the collinear points.
- 2. The fate of a small displacement on a test particle located at each point.
- 3. Stability region versus the mass ratio for each point.

The initial conditions of the orbit of the primaries can be found in Abd El-Bar et al. (2015). Eccentricity = 0.2, semimajor axis =1.1, square of mean motion = 0.96714015, true anomaly = 0 degree and $\mathcal{F} = (1/1.2)$. In addition to the following domains of the perturbing parameters tabulated in the following Table 1.

In what follows, we gave some plots to illustrate and interpret the difference between the locations of L_i , i =1, 2, 3 in the classical CRTBP and in the perturbed ERTBP.

Table 1. Small parameters of different included perturbations

Larger primary	Smaller primary	
Oblateness	$A_1 \in]0, 0.01]$	$A_2 \in]0, 0.001]$
Triaxiality	$(2\sigma_1-\sigma_2)\in$	$(2\gamma_1-\gamma_2)\in$
]0, 0.0018]]0, 0.0014]
Total perturbations	$A_{\sigma} \in \left]0, 0.0118\right]$	$A_{\gamma} \in]0, 0.0024]$

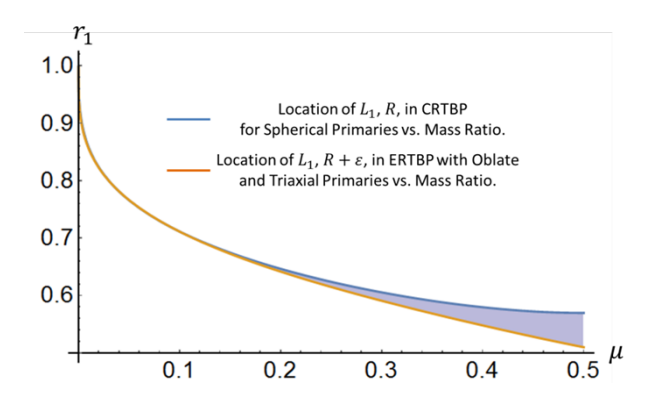


Figure 1. Location of vs. for two different cases, CRTBP for spherical primaries and ERTBP with oblate and triaxial primaries.

In Figures 1, 4, 7 we plotted the locations of L_i , i = 1, 2, 3 versus the whole mass ratio $\mu \in]0, 0.5]$.

In Figure 1 the location decreases with increasing the mass ratio, *i.e.* the equilibrium point L_1 moves left towards the barycenter. In Figure 7 the location decreases with increasing the mass ratio, *i.e.* the equilibrium point L_1 moves right towards the barycenter. This may be attributed mainly to the gravitational field of the massive primary. The size of perturbation between the classical CRTBP and in the perturbed ERTBP in determination of the location of L_1 and L_3 become significant and noticeable for larger mass ratios, approximately $\mu > 0.25$. The gravitational fields of the primaries in both case illustrated in Figure 1 and in Figure 7 have only one line of action towards the left at L_1 and towards the right at L_3 . This may interpret well the decreasing nature of the curves obtained in Figure 1, 7.

In **Fig. 4** the location increases with increasing the mass ratio, *i.e.* the equilibrium point L_2 moves right towards the les massive object away from the barycenter, which is very difficult to be interpreted but it may partially attributed due to close vicinity of L_2 to the less massive primary and the gravitational fields of the primaries have two inverse lines of action at L_2 , to the left towards the massive body and to the right towards the less massive one. Therefore the gravitational field of the less massive body will be more effective at L_2 than the gravitational field of the massive primary. Also the rotating frame may give a contribution to the effect.

The size of perturbation between the classical CRTBP and in the perturbed ERTBP in determination of the location of L_2 is very tiny. This may support our interpretation that we are very colse to the less massive primary.

In Figures 2, 5, 8 small displacement leads to departure which enhances the instability of L_i , i = 1, 2, 3 illustrated in Figures 3, 6, 9. The only difference is the velocity of departure from equilibrium point.

According to Eq. (13, 14, 15), the characteristic equations of L_i , $i=1,\ 2,\ 3$ of ERTBP for $\mu=0.01$ are respectively given by

$$\lambda^4 - 3.51423 \ \lambda^2 - 45.2287 = 0 \tag{36}$$

$$\lambda^4 - 0.698 \,\lambda^2 - 11.13 = 0 \tag{37}$$

$$\lambda^4 - 1.4677 \ \lambda^2 - 0.020171 = 0 \tag{38}$$

From Eq. (12), Eq. (16), Eq. (36), Eq. (37), and Eq. (38) we have the following sets

For L_1

$$\mathcal{X} = 10^{-6} \times \left[6.95 \ e^{-2.95 \ f} + 5.03 \ e^{2.95 \ f} \right]$$

$$-1.98 \cos(2.28 \ f) + 2.49 \sin(2.28 \ f)$$

$$\mathcal{Y} = 10^{-6} \times \left[3.24 \ e^{-2.95 \ f} - 2.35 \ e^{2.95 \ f} \right]$$

$$+9.1 \cos(2.28 \ f) + 7.24 \sin(2.28 \ f)$$

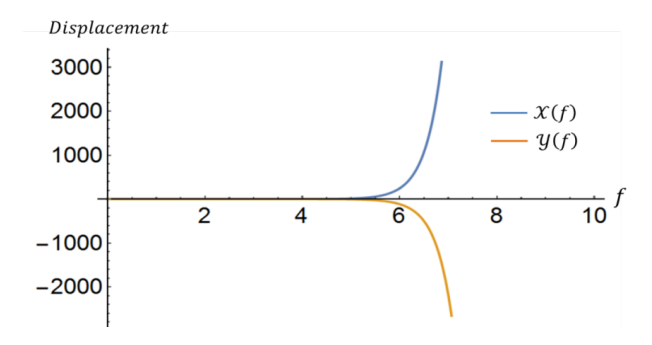


Figure 2. The growth of a small displacement for a test particle placed at L_1 vs. f.

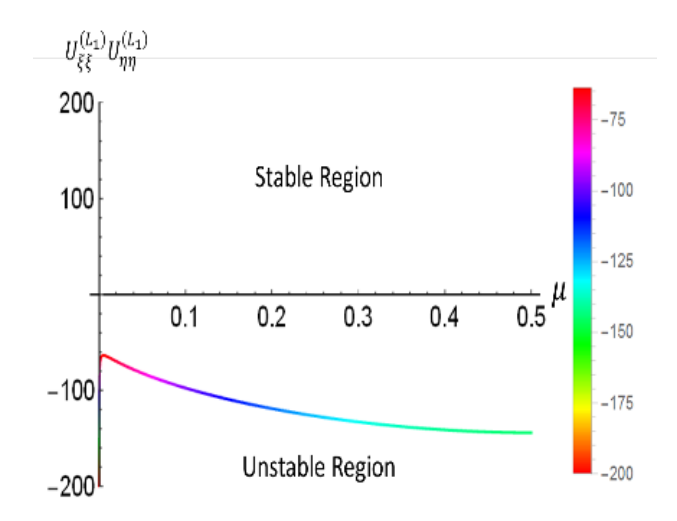


Figure 3. Stability region vs. μ for L_1 for ERTBP with oblate and triaxial primaries.

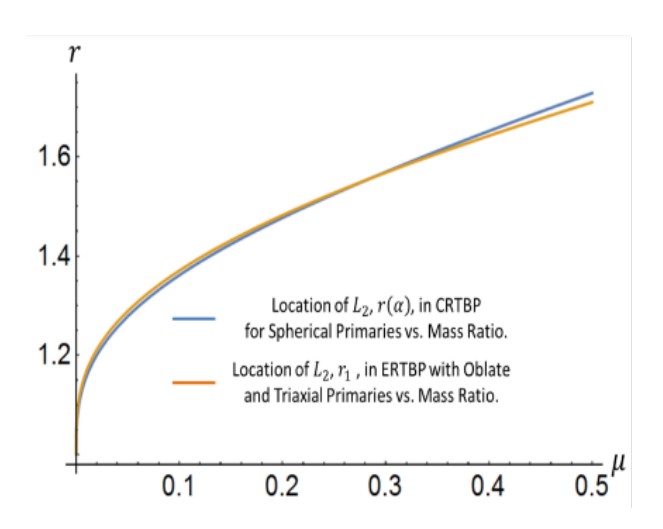


Figure 4. Location of L_2 vs. μ for two different cases, CRTBP for spherical primaries and ERTBP with oblate and triaxial primaries.

For L_2

$$\mathcal{X} = 10^{-6} \times \left[8.37 \ e^{-1.92 f} + 5.69 \ e^{1.92 f} \right]$$

$$-4.06 \cos (1.73 f) + 2.98 \sin (1.73 f)$$

$$\mathcal{Y} = 10^{-6} \times \left[5.93 \ e^{-1.92 f} - 4.03 \ e^{1.92 f} \right]$$

$$+8.1 \cos (1.73 f) + 11.1 \sin (1.73 f)$$
(40)

For L_3

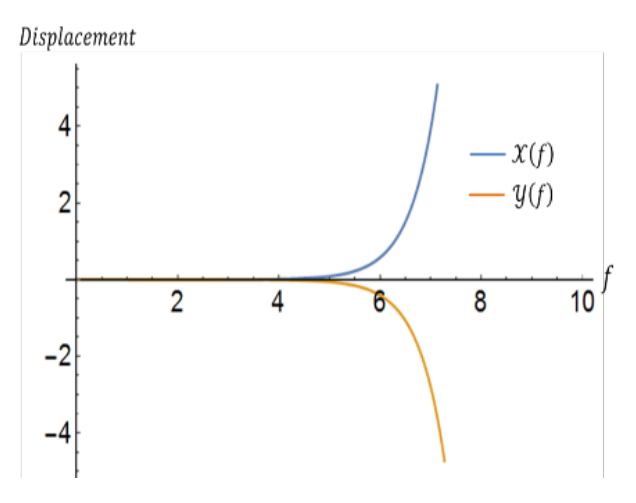


Figure 5. The growth of a small displacement for a test particle placed at L_2 vs. f.

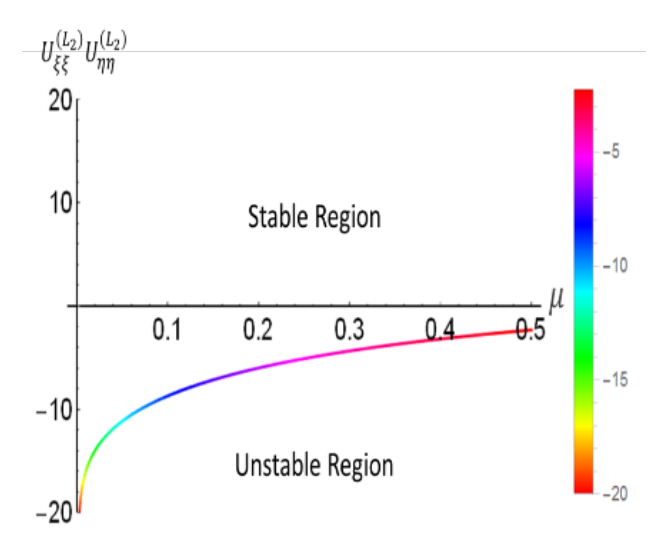


Figure 6. Stability region vs. μ for L_2 for ERTBP with oblate and triaxial primaries.

$$\mathcal{X} = 10^{-6} \times \left[13.9 \ e^{-0.117 f} + 13 \ e^{0.117 f} \right]$$

$$-16.9 \cos (1.22 f) + 8.73 \times 10^{-2} \sin (1.22 f)$$

$$\mathcal{Y} = 10^{-6} \times \left[151 \ e^{-0.117 f} - 141 \ e^{0.117 f} \right]$$

$$+0.144 \cos (1.22 f) + 27.9 \sin (1.22 f)$$
(41)

It is clear that the first term is a decay and the third and fourth is an oscillation while the second term represents a growth that is the source of unstable case for L_1 and it dominates all other terms, see Figures 2, 5, 8. The

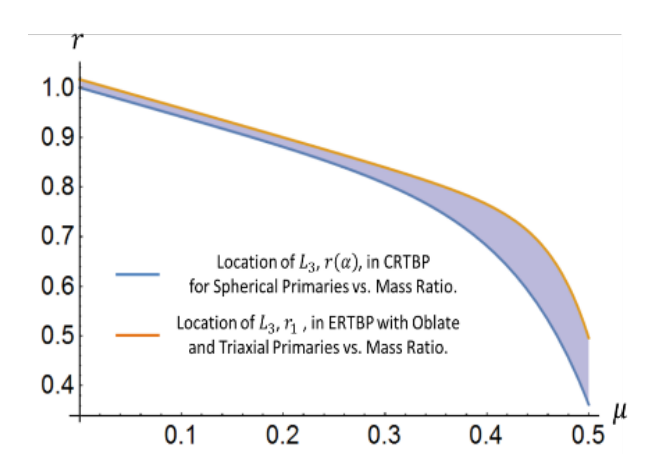


Figure 7. Location of L_3 vs. μ for two different cases, CRTBP for spherical primaries and ERTBP with oblate and triaxial primaries

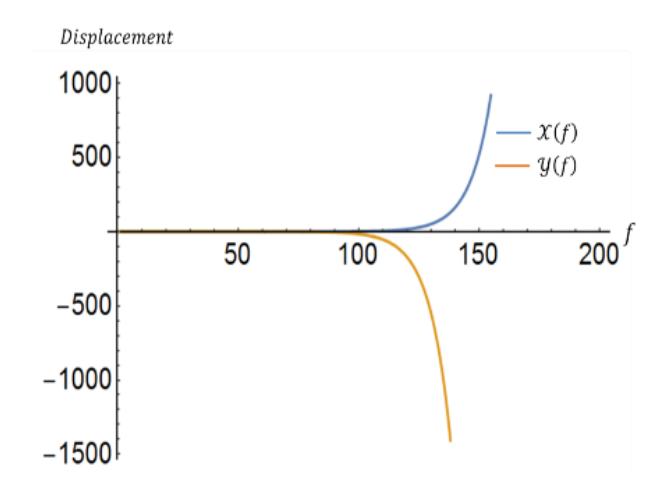


Figure 8. The growth of a small displacement for a test particle placed at L_3 vs. f.

value of the constant term in the characteristic equation is always negative overall $0 < \mu \le \frac{1}{2}$. This implies that the first condition of stability is not achieved. See Figures 3, 6, 9.

7 Conclusion

We have considered the ellipticity, oblateness and triaxiality perturbations as a modification to the classical CRTBP. These perturbations as expected bring deviations of the locations of the equilibrium points from classical CRTBP. In this work, we computed and illustrated these deviations in collinear points explicitly as functions in the mass ration. We investigated the stability of the collinear equilibrium points. The absolute deviation in the location of all collinear points is the ratio between the first partial derivative of the

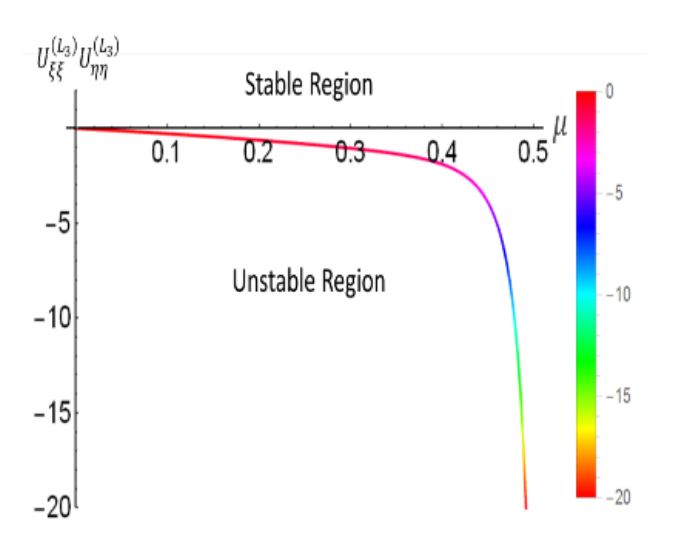


Figure 9. Stability region vs. μ for L₃ for ERTBP with oblate and triaxial primaries.

potential-like function to the second partial derivative of the same function with respect to ξ axis at the solution of classical CRTBP. In all collinear points, the size of perturbations coming from the different perturbing sources are almost comparable at small and moderate mass ratios, But this becomes distinguishable for late moderate and high mass ratios. Also in all cases, the equilibrium points undergo instabilities in the whole domain of mass ratio.

Acknowledgment: The authors appreciate the supportive suggestions of the editor and Referees which improved the quality of the manuscript.

References

Abd El-Bar, S. E., Abd El-Salam, F. A., Rassem, M. 2015, Canad. J. Phy., 93(3), 300-311.

Abd El-Salam, F. A., 2015 Astrophys Space Sci. 357(1), 15. doi: 10.1007/s10509-015-2308-5

Abd El-Salam, F. A., Abd El-Bar, S. E. 2019, Canadian Journal of Physics. 97(3), 231-240.

Abd El-Salam, F. A., Abd El-Bar, S. E. 2015, Phys. J. Plus. 130, 234. Doi: doi:10.1140/epjp/i2015-15234-x

Ammar, M.K. 2008, Astrophys. Space Sci. 313(4), 393-408.

Bello, Nakone, Singh, Jagadish. 2016, 57(2), 576-587.

Kushvah, B. S. & Ishwar, B. 2004, Review Bull.Cal. Math. Soc.12 (1 & 2), 109-114.

Katour, D.A., Abd El-Salam, F.A. & Shaker, M.O. 2014, Astrophys Space Sci. 351(1), 143-149.

Kumar, S. & Ishwar, B. 2009, In: Proceedings of the International Conference on Modelling and Engineering and Technological Problems, ICMETR'09, AIP Conference Proceedings, 1146, 456-461. Mital, A., Ahmad, I., Bhatnagar, K.B. 2009, Astrophys. Space Sci. 323, 65-73.

Murray, C. & Dermott, S. 1999, Solar System Dynamics. Cambridge University Press, Cambridge.

Rahoma, W. A., Abd El-Salam, F. A. 2014, J. of Astron. and Space Sci. 31(4), 285-294.

Rahoma, W. A. 2016, J. of Astron. and Space Sci. 33(4), 257-264.

Sharma, R.K. 1987, Astrophys. Space Sci. 135, 271.

Sharma, R.K., Taqvi, Z.A., Bhatnagar, K.B. 2001, Celest. Mech. Dyn. Astron. 79, 119-133.

Singh, J. & Ishwar, B. 1999, Bull. Astron. Soc. India, 27, 415-424.

Singh, J. 2011, Astrophys. Space Sci. 332(2), 331-339.

Singh, J. & Umar, A. 2012, Astrophys. Space Sci. 341, 349-358.

Singh, J. & Umar, A. 2012, AJ, 143, 109-131.

Singh, J. & Umar, A. 2013, Astrophys Space Sci. 348(2), 393-402.

Singh, J. & Umar, A. 2013, Advances in Space Research 52(8), 1489-1496.

Singh, J. & Umar, A. 2013, Astrophys Space Sci., 344(1), 13-19.

Singh, J. & Umar, A. 2014, New Astron., 29, 36-41.

Singh, J. & Bello, N. 2014, Astrophys Space Sci., 351(2), 491-497.

Singh, J. & Bello, N. 2014, Astrophys Space Sci., 351(2), 483-490.

Singh, J. & Bello, N. J. 2014, Astrophys Astron. 35(4), 701-713.

Singh, J. & Bello, N. 2015, Adv. in Astron., Article Id: 489120. Doi: doi.org/10.1155/2015/489120.

Szebehely, V. 1967, Theory of Orbits. Academic Press, New York. Tsirogiannis, G.A., Douskos, C.N., Perdios, E.A. 2006, Astrophys. Space Sci. 305, 389.

Vishnu Namboori, N.I., Reddy, D.S., Sharma, R.K. 2008, Astrophys. Space Sci., 318, 161.

Wang, X., Wu, N., Zhou, L., Xu, B. 2018, arXiv:1803.06614v1.

Xin, X., Hou, X. 2017, AJ, 154(37), 10. Doi: 10.3847/1538-3881/aa774fD

Wu, N., Wang, X., Zhou, L., Xu, B. 2018, A&A, 614, A67.